

1 **Salinity changes and anoxia resulting from enhanced runoff**
2 **during the late Permian global warming and mass extinction**
3 **event**
4

5 Elsbeth E. van Soelen¹, Richard J. Twitchett², Wolfram M. Kürschner¹
6

7 ¹University of Oslo, Departments of Geosciences, P.O box 1047 Blindern 0316 Oslo, Norway
8

9 ²Natural History Museum, Earth Sciences Department, London, SW7 5BD, UK
10

11 *Correspondence to:* Elsbeth E. van Soelen (e.e.v.soelen@geo.uio.no)

Abstract. The Late Permian biotic crisis had a major impact on marine and terrestrial environments. Rising CO₂ levels following Siberian Trap volcanic activity were likely responsible for expanding marine anoxia and elevated water temperatures. This study focuses on one of the stratigraphically most expanded Permian-Triassic records known, from Jameson land, east Greenland. High-resolution sampling allows for a detailed reconstruction of the changing environmental conditions during the extinction event and the development of anoxic water conditions. Since very little is known about how salinity was affected during the extinction event, we especially focus on the aquatic palynomorphs and infer changes in salinity from changes in the assemblage and morphology. The start of the extinction event, here defined by a peak in spore/pollen, indicating disturbance and vegetation destruction in the terrestrial environment, postdates a negative excursion in the total organic carbon, but predates the development of anoxia in the basin. Based on the newest estimations for sedimentation rates, the marine and terrestrial ecosystem collapse took between 1.6 to 8 kyrs, a much shorter interval than previously estimated. The palynofacies and palynomorph records show that the environmental changes can be explained by enhanced runoff, increased primary productivity and water column stratification. A lowering in salinity is supported by changes in the acritarch morphology. The length of the processes of the acritarchs becomes shorter during the extinction event and we propose that these changes are evidence for a reduction in salinity in the shallow marine setting of the study site. This inference is supported by changes in acritarch distribution, which suggest a change in palaeoenvironment from open marine conditions before the start of the extinction event to more near-shore conditions during and after the crisis. In a period of sea-level rise, such a reduction in salinity can only be explained by increased runoff. High amounts of both terrestrial and marine organic fragments in the first anoxic layers suggest that high runoff, increased nutrient availability, possibly in combination with soil erosion, are responsible for the development of anoxia in the basin. Enhanced runoff could result from changes in the hydrological cycle during the late Permian extinction event, which is a likely consequence of global warming. In addition, vegetation destruction and soil erosion may also have resulted in enhanced runoff. Salinity stratification could potentially explain the development of anoxia in other shallow marine sites. The input of fresh water and related changes in coastal salinity could also have implications for the interpretation of oxygen isotope records and seawater temperature reconstructions in some sites.

1. Introduction

The late Permian extinction event was the most severe global crisis of the Phanerozoic in terms of both taxonomic loss and ecological impact (e.g. McGhee et al., 2012). The current consensus is that the extinction was likely due to global warming and associated environmental changes caused by CO₂ emissions from Siberian Trap volcanic activity, because of the close timing between the volcanic activity and the extinction event (e.g., Burgess et al., 2017; Burgess and Bowring, 2015). Most studies on the late Permian extinction have inferred that expanding marine anoxia (e.g. Wignall and Hallam, 1992) is a key biotic factor causing marine extinction and ecosystem collapse. There are different theories to explain the spreading of anoxia, which affected both deep and shallow sites (e.g. Bond and Wignall, 2010; Isozaki, 1997; Wignall and Twitchett, 1996). A weakened temperature gradient between equator and pole would have slowed ocean circulation and may have facilitated expansion of the oxygen minimum zone (Hotinski et al., 2001). Increased weathering and detrital input (Algeo and Twitchett, 2010), and soil erosion (Sephton et al., 2005) led to enhanced terrestrial matter input in marine sections, and may also have contributed to eutrophication and in stratified waters led to hypoxia or anoxia (Sephton et al., 2005). Other factors that are thought to play important roles in the extinction are elevated water temperatures (e.g. Sun et al., 2012), and ocean acidification (Clapham and Payne, 2011). One important environmental parameter that has received relatively little attention is salinity, even though low salinity ocean conditions were once considered to be a leading cause of the marine extinction (Fischer, 1964; Stevens, 1977). Furthermore, potential impacts of changes in salinity, which might be expected from enhanced discharge of freshwater into shelf seas (Winguth and Winguth, 2012), have been largely ignored.

Microfossils of marine algae are excellent recorders of environmental change in the water column. Of these, the organic-walled cysts of dinoflagellates have proven especially useful in palaeo-environmental studies (e.g. Ellegaard, 2000; Mertens et al., 2009, 2012, Mudie et al., 2001, 2002; Sluijs and Brinkhuis, 2009; Vernal et al., 2000). While dinocysts are absent or sparse in Palaeozoic deposits, acritarchs are commonly recorded (e.g. Tappan and Loeblich, 1973), even during the late Permian when acritarch diversity was declining (Lei et al., 2013b). Acritarchs are a group of microfossils of organic composition and unknown affinity (Evitt, 1963). Many acritarchs are, however, considered to be phytoplankton, and some are thought to be precursors of modern dinoflagellate cysts (e.g. Lei et al., 2013b; Servais et al., 2004). Several studies in East Greenland have reported fluctuating abundances of acritarchs during the Late Permian and Early Triassic (e.g. Balme, 1979; Piasecki, 1984; Stemmerik et al., 2001), but very few late Permian studies have documented the relative abundance of the different genera of aquatic palynomorphs (for example, Shen et al., 2013). Similar to dinocysts, acritarch morphology has been linked to environmental conditions, and acritarchs with longer processes are generally more abundant in more open marine settings (Lei et al., 2012; Stricanne et al., 2004). Both dinocyst and acritarch studies show that salinity might be an important factor that influences cyst morphology (Servais et al., 2004). It is thought that the longer processes in higher salinities stimulate clustering with other cysts or particles in the water column, and thus enhance sinking to the seafloor (Mertens et al., 2009).

The rock record of Jameson Land, East Greenland, has provided key insights into marine environmental changes during the late Permian extinction event. Previous work on this section by Twitchett et al. (2001) showed that collapse of marine and terrestrial ecosystems was synchronous and took between 10 to 60 kyr. Palynological work by Looy et al. (2001) showed that the terrestrial ecosystem collapse is characterized by a

distinct rise in spores, indicative of the loss of woodland and increase in disturbance taxa. The onset of anoxic conditions is not as abrupt at this location as seen in some other sections, but instead Wignall and Twitchett, (2002) found unusual alternating patterns of bioturbated and laminated siltstones in the top of the Schuchert Dal Formation and lowest of the Wordie Creek Formation (Fig. 1). In a recent study, Mettam et al., (2017) showed that rapidly fluctuating redox conditions occurred during the late Permian extinction, while sedimentological observations imply that sea level was rising in this period. Estimations of sedimentation rates indicate that each bioturbated/laminated rock interval, which are between 2-10 cm thick, have been deposited in a period of 50-1000 years (Mettam et al., 2017). To study the environmental conditions associated with the deposition of these sediments we look in detail at a short (9 m) interval covering the late Permian extinction and the Formation boundary between the Schuchert Dal and Wordie Creek Formation. Palaeoenvironment is studied by looking at variations in the palynofacies (organic particles) and the acritarch assemblage. In addition we present a record of morphological changes within the acritarch *Micrhystridium*. Runoff and erosion, salinity, sea-level fluctuations and temperature rise are discussed as possible reasons for the changing environmental conditions.

2. Geological setting and stratigraphy

Samples were collected at the Fiskegrav location of Stemmerik et al. (2001), an outcrop in East Greenland (N71°32'01.6", W024°20'03.0"), in a small stream section on the east side of Schuchert Dal (Fig. 1). The section was deposited within a relatively narrow, north-south oriented basin (Stemmerik et al., 2001; Wignall and Twitchett, 2002). Active rifting and rapid subsidence has resulted in the deposition of one of the most expanded P-Tr sections. At the Fiskegrav location there are no obvious breaks in sedimentation, even though large erosive channels exist in P-Tr sections in more northern locations (Twitchett et al., 2001; Wignall and Twitchett, 2002).

The Fiskegrav section shows a transition from the Schuchert Dal Formation into the Wordie Creek Formation. The Permian/Triassic boundary, defined by the first occurrence of the conodont *Hindeodus parvus* (Yin, 1996), is located at 23.5 m above the base of the Wordie Creek Formation (Twitchett et al., 2001). This study focuses on a ca. 9 m section interval including the late Permian extinction and the formation boundary (Fig. 1). The upper part of the Schuchert Dal Formation consists of blocky (bioturbated), micaceous, greenish mudstones (muddy siltstones), whereas the lower Wordie Creek Formation consists mainly of laminated, dark grey mudstones (clay-siltstones) that often contain framboidal pyrite (Twitchett et al., 2001; Wignall and Twitchett, 2002). The extinction event occurs in the upper metres of the Schuchert Dal Formation, and the start of the biotic crisis is synchronous in marine and terrestrial ecosystems (Looy et al., 2001; Twitchett et al., 2001). For more details on biostratigraphy see Mettam et al., (2017); Stemmerik et al., (2001) and Twitchett et al., (2001).

3. Material and Method

3.1 Material

A total of 36 samples were collected from the top 4.5m of the Schuchert Dal Formation and the lower 4.2m of the Wordie Creek Formation. Sample resolution is highest (10cm intervals) in the 2.5m interval covering the formation boundary and the extinction event. Depths are given in m, relative to the formation boundary between Schuchert Dal and Wordie Creek Fm. Some of the samples used in this study were also analysed by Mettam et al. (2017) during their study of changes in redox conditions at the formation boundary.

3.2 palynofacies and palynological analysis

Samples (of ca.5 g) were crushed, and a tablet with a known amount of lycopodium spores was added to allow quantification of organic particles and palynomorphs. Samples were then treated with hydrochloric acid and hydrofluoric acid to remove carbonates and silicates, and subsequently sieved through 7 µm sieves. Heavy liquid separation was used to remove heavy minerals like pyrite. The residue, containing palynomorphs and other organic particles, was mounted onto microscope slides. Material was counted using a Leitz Diaplan microscope and an AxioCam ERc 5s camera attached to a computer with Zen microscope software (Zen 2 lite, 2011). A minimum of 300 particles per sample were counted for palynofacies analyses. Aquatic palynomorphs were counted to reach 100 specimens when abundant and at least 30 specimens when abundance was low. Still, due to low abundances during the biotic crisis, in some samples counts were below 30 (these 6 samples are indicated in Fig. 4).

3.3 Acritarch measurements

The genus *Michrhystridium* includes many species, of which ca. 20 are known from the Permian-Triassic interval, which differ in their body size, number of processes and process length (Lei et al., 2013b; Sarjeant, 1970). Only those with a spherical central body and many (>10) simple processes with closed tips were included in this study (i.e. the *M. breve* Group, according to Lei et al., 2013b). Thus, amongst others, *M. pentagonale* was excluded. Specimens were excluded if they were too damaged (folded or broken) to allow measurements. To counteract the effects of compression (which can make the body look longer), body size was calculated from the average of two linear measurements perpendicular to each other. The choice of processes was limited due to compaction of the acritarchs. If more than 3 processes were available for measurement, a focal plane was chosen that showed most, and best preserved processes, from which we measured the three longest, following the methodology by Mertens et al., (2012). The aim was to measure 20-30 specimens per sample, but acritarch concentrations were low during the biotic crisis interval, and therefore 5 samples had lower counts (indicated in Fig. 6).

4. Results

4.1 Palynofacies

The most abundant organic particles are phytoclasts and amorphous organic matter (AOM) which together comprise 45 to 90% of the palynofacies (Fig. 2). Phytoclasts are dominant in the bioturbated samples in the lower part of the section, while AOM dominates the palynofacies in the laminated intervals. Other terrestrially derived organic (wood fragments and charcoal) particles make up a small portion (<20%) of the palynofacies and are not influenced by the alternating anoxic/oxic depositional conditions (Fig. 2). Palynomorphs were divided into three groups: pollen, spores and aquatic palynomorphs. Pollen abundance relative to other palynofacies is higher in the upper 0.5 m of the Schuchert Dal Formation and lowest metre of the Wordie Creek Formation (5-20%), which is mainly caused by the high number of pollen fragments (sacci) during and following the extinction event (Fig. 2). Spores have highest abundance in the upper metre of the Schuchert Dal Formation (up to 35%), where also the spore/pollen ratio is highest. Aquatic palynomorphs (acritarchs and other algal remains like *Tasmanites* and *Cymatiosphaera*) make up a very small fraction of the palynofacies in the Schuchert Dal Formation (<2%), but become relatively more abundant in the Wordie Creek Formation (up to 14%).

4.2 Aquatic palynomorphs

Although Permian acritarch diversity is considered to be low, an overview of Permian phytoplankton by Lei et al. (2013b) showed a richness of about 20-30 genera during most of the Permian, with acritarchs belonging to the genera *Micrhystridium* and *Veryhachium* being the most common (Lei et al., 2013b, 2013a; Sarjeant and Stancliffe, 1994). Since cysts are generally small in size it is difficult to study them under light microscope and identification at species level can be difficult (Sarjeant, 1970). Several revisions and simplifications have been proposed for the genera (Lei et al., 2013a; Sarjeant and Stancliffe, 1994). We follow the simple classification scheme proposed by Lei et al. (2013a), in which different species of acritarchs are grouped together, based on geometrical shape of the acritarchs. Photos of selected aquatic palynomorphs are shown in the plate of Fig. 3.

Concentrations of aquatic palynomorphs were on average ca.4 times higher in the laminated rocks compared to the bioturbated rocks (Fig. 4). Acritarch abundance also declines during the extinction event. The majority (25 - 100%) of the acritarchs belong to the *Micrhystridium breve* Group (Fig. 4). This group includes all acritarchs with a spherical central body and numerous processes. The *Veryhachium laidii* Group (acritarchs with a rectangular central body shape), the *V. trispinosum* Group (triangular shape), *V. cylindricum* Group (ellipsoidal shape) and *M. pentagonale* Group (pentagonal or hexagonal shape) were mostly found in bioturbated intervals of the upper part of the Schuchert Dal Formation, especially just before and during the extinction interval (Fig. 4). The leiospheres include all aquatic palynomorphs with a spherical shape and either a smooth surface or with small ornamentation, but no processes. The highest abundances (up to 70%) of leiospheres are found in the laminated sediments of the Wordie Creek Formation (Fig. 4). *Cymatiosphaera* are rare in the record and found in both the oxidized siltstones of the Schuchert Dal Formation, but also in some intervals in the laminated siltstones. *Tasmanites* were found only in one sample, also during the marine extinction phase. The apparent relatively higher abundance of *Cymatiosphaera* and *Tasmanites* in the top of the Schuchert Dal Formation is a consequence low total count of the aquatic palynomorphs during the extinction

event. The most diverse samples were found in the bioturbated rocks of the upper metre of the Schuchert Dal Formation, an interval that partly overlaps with the extinction interval.

The *Micrhystridium* Group has a diverse morphology, and shows variation in vesicle size and number of processes. Most of the measured specimens are very similar to the species *M. breve* as described by Jansonius (1962) in both the number and shape of the processes. However, the size of the central body and the length of the processes of many of the measured acritarchs fall outside of the defined size-range of *M. breve*. Variability in process length within one specimen was generally small (in almost 80% of the specimen measured $<2\mu\text{m}$) and in only 7% of the cases $>3\mu\text{m}$) (see also table S4). The distributions of both body size and process length are unimodal (Fig. 5), which suggests that the measured specimens all belong to a single species of *Micrhystridium*. Body size is variable, with a decrease around -150cm from 16.5 to $13.5\mu\text{m}$, followed by a gradual increase throughout the extinction event up to $19\mu\text{m}$ at 75cm, followed by an abrupt decrease to $14\mu\text{m}$, after which body size stabilizes between 14.5 and $16\mu\text{m}$. In the two-metre interval spanning the formation boundary, acritarchs in the laminated rocks are on average larger compared to those in the bioturbated rocks, however, this is not consistently true further up or down the section (Fig. 6). The average process length first increases before the start of the extinction from an average 7.7 at -450cm to $11.5\mu\text{m}$ at -250cm , after which processes gradually become shorter down to a minimum of around $5\mu\text{m}$ during the extinction event. Processes then remain shorter through to the top of the studied section. Process length not only changes in absolute terms, but also relatively to the size of the body.

5. Discussion

5.1 The extinction event and onset of anoxia

Consistent with the results of Looy et al. (2001), we find a strong increase in spores, relative to pollen, in the upper Schuchert Dal Formation (Fig. 2). Since this peak in spores coincides with the interval of marine ecosystem collapse defined by Twitchett et al. (2001), we define the period with highest spore/pollen ratios as the extinction interval. Twitchett et al. (2001) found large changes in marine plankton abundance in their study of the Fiskegrav section, with a bloom just before the disappearance of trace fossils, followed by almost complete absence of acritarchs immediately after the collapse of the marine ecosystem. This phytoplankton bloom is not obvious in our higher resolution data, and may simply be an artefact of the relatively low-resolution sampling of Twitchett et al., (2001), but the number of acritarchs is indeed greatly reduced during the biotic crisis (Fig. 4). The peak in spore/pollen and decrease in acritarch abundance occurs in an interval of ca. 0.8m , which is comparable to the interval found by Twitchett et al., (2001) for marine and terrestrial ecosystem collapse. Twitchett et al., (2001) estimated the collapse to have taken between 10 and 60 kyrs, however, recently improved estimations of sedimentation rates in the Fiskegrav section (Mettam et al 2017) now give an estimated duration of between 1.6 to 8 kyrs for the marine and terrestrial ecosystem collapse.

During the start of the biotic crisis rocks remain bioturbated but within the upper 0.5 m of the Schuchert Dal Formation there are intervals with laminated rocks (Fig. 2), indicative for anoxia (Twitchett et al., 2001). AOM, which is structureless organic matter, is dominant in the laminated rocks. AOM can derive from

degraded macrophyte, phytoplankton or higher plant tissue, or it may also be bacterially derived (Tyson, 1995). Anoxic conditions can stimulate the production of marine AOM (Pacton et al., 2011), but also result in better preservation after sedimentation (Tyson, 1995). The relative proportions of AOM versus phytoclasts thus indicate the amount of oxygenation of the depositional environment (Tyson, 1995). A recent, high-resolution study of the $\delta^{13}\text{C}$ of total organic carbon (TOC) by Mettam et al., (2017) shows a negative shift of 5-6‰ that begins 1.80m below the top of the Schuchert Dal Formation at Fiskegrav, (Fig. 2). The onset of this negative excursion coincides closely with the last occurrence of Permian macroinvertebrate fossils (Mettam et al., 2017), but pre-dates the collapse of marine and terrestrial ecosystems defined by disappearance of bioturbation. Mettam et al. (2017) record a small, but consistent, offset in $\delta^{13}\text{C}$ values between the laminated/bioturbated intervals (Fig. 2). This offset can be explained by the differences in organic matter source, which is mostly phytoclasts (terrestrial) in the bioturbated intervals while AOM (marine and terrestrial) dominates in the laminated intervals. However, the main shift is not associated with major changes in the palynofacies, and occurs in a part of the section where the palynofacies mainly consist of terrestrially derived organic matter (Fig. 2). This negative shift in carbon isotopes associated with the late Permian extinction event is recognized worldwide (e.g. Korte and Kozur, 2010) and usually precedes, the extinction event (e.g. Burgess and Bowring, 2015; Korte and Kozur, 2010). It has been interpreted as resulting from atmospheric changes in $\delta^{13}\text{C}$ values, which can be directly, or indirectly, related to Siberian trap volcanism (e.g. Cui and Kump, 2015; Svensen et al., 2009).

Mettam et al. (2017) studied redox conditions in the same section and showed that conditions became potentially anoxic, and ferruginous (Fe^{2+} - rich) in the laminated intervals near the formation boundary. Within the lowermost Wordie Creek Formation, from 0.6-0.7 m above the formation boundary, anoxic conditions are confirmed by Fe speciation (Mettam et al., 2017). Since the extinction started before conditions became ferruginous, spreading anoxia cannot be the main cause for the marine biotic crisis in the Fiskegrav section. Grasby et al. (2015) distinguished three phases of extinction in the shallow marine sequence of Festningen (Svalbard): first is the loss of carbonate macrofauna, followed by loss of siliceous sponges, and finally a loss of all trace fossils. Thus, similar to what is observed in East Greenland, the first laminated sediments do not represent the start of the biotic crisis. This is unsurprising as expanding marine hypoxia is a predicted consequence of global warming, which was probably caused by elevated CO_2 flux from Siberian Trap volcanism (Benton and Twitchett, 2003; Grard et al., 2005). Therefore, extinctions that occurred prior to the appearance of widespread anoxia were more likely due to the direct, short-term effects of volcanic activity (e.g. metal toxicity), or the more immediate effects of CO_2 rise or temperature increase. The laminated rocks are associated with higher amount of pollen fragments (Fig. 2), which could be an indication for elevated terrestrial organic matter input (e.g. soil erosion), while the higher amount of AOM can be partly explained by terrestrial organic matter input, and partly by increased marine productivity and better preservation of organic matter due to low oxygen conditions. Increased weathering and run-off are expected consequences of atmospheric and hydrological changes associated with global warming. Algeo and Twitchett, (2010) demonstrated that sediment accumulation rates greatly increased in shallow shelf seas in the latest Permian and earliest Triassic, consistent with enhanced weathering and run-off, and Sephton et al. (2005) found evidence for large-scale soil erosion.

5.2 Sea-level and salinity changes

If the laminated rocks are indeed a consequence of enhanced runoff, this is expected to affect also marine environmental conditions, such as a decrease in (surface) salinity. At the same time, sea-level fluctuations at and near the boundary need to be considered, since these would also affect marine environmental conditions and could potentially affect salinity. The Fiskegrav section has well preserved aquatic palynomorphs, and their diversity, distribution and morphology can provide valuable information on marine environmental changes. Palaeozoic studies have shown that acritarch diversity is generally higher in deeper, more distal settings (e.g. Lei et al., 2012; Stricanne et al., 2004). In addition, different studies have shown that *Veryhachium* favoured more open marine settings, while *Micrhystridium* favoured near-shore environments (e.g. Wall 1965, Lei et al., 2012). It is possible that some of the leiospheres in the Fiskegrav section belong to the genus *Leiosphaeridia*, as the dimensions are comparable to *L. microgranifera* and *L. minutissima* that were found in Chinese Permian-Triassic sections (Lei et al., 2012), but the small ornamentations on both of those species is different (Fig. 3). In these Chinese Permian sections the *Leiosphaeridia* are associated with deeper/more open marine waters (Lei et al., 2012). On the other hand, studies of early Palaeozoic acritarchs show that, in general, leiospheres, or sphaeromorphs, are most frequent in proximal environments (Li et al., 2004; Stricanne et al., 2004). The leiosphere-group might be polyphyletic and some species might have prasinophyte affinities (Colbath and Grenfell, 1995), which complicates their use for environmental reconstructions. Whatever the biological origin of the leiosphere is, in this study site they apparently favoured the palaeoenvironmental conditions associated with the deposition of the laminated rocks, starting during the extinction event.

In the Fiskegrav section, the decline in diversity from the upper Schuchert Dal Formation to the Wordie Creek formation, together with the change in assemblage from *Veryhachium*/*Micrhystridium* to *Micrhystridium*/leiosphere dominance could thus be interpreted as a change from a distal to a more proximal setting, which would suggest a marine regression. Although this was once considered as a possible cause of the late Permian extinction event (Hallam and Cohen, 1989), the current consensus is that eustatic sea-level fall occurred prior to collapse of marine ecosystems and the extinction, and the subsequent transition from the Permian to the Triassic happened during sea-level rise (Wignall and Hallam, 1992). In some East Greenland locations, apparently missing biozones and local erosive conglomeratic channels have been proposed as evidence for sea-level fall near the boundary between the Schuchert Dal and Wordie Creek formations (Surlyk et al., 1984), but Wignall and Twitchett (2002) demonstrated that in central Jameson Land the sedimentological changes are consistent with sea-level rise, and that the erosive, conglomeratic channels occur at multiple stratigraphic levels and postdate the extinction and Permian/Triassic boundary.

Thus, during the extinction event the acritarch assemblage changes to a more typical near-shore assemblage, despite the ongoing sea-level rise. Instead of a marine regression, the observed shift in acritarch assemblages could be explained by an increase in runoff which affects the near-shore environment by lowering surface water salinity and delivering nutrients, both of which are found to affect the distribution of modern phytoplankton (e.g. Bouimetarhan et al., 2009; Devillers and de Vernal, 2000; Pospelova et al., 2004; Zonneveld et al., 2013). Dinocyst morphology has also been linked to environmental conditions (e.g., Mertens et al., 2009, 2011), with salinity identified as an important factor influencing process length (Ellegaard et al., 2002; Mertens et al., 2011). Similarly, studies of acritarch process length and palaeoenvironment show that species and individuals with longer processes are generally found in more offshore locations, while in inshore settings

acritarchs with shorter processes are more abundant (Lei et al., 2013a; Servais et al., 2004; Stricanne et al., 2004). The average process length of specimens belonging to the *Micrhystridium breve* -group, show a decreasing trend during the extinction interval, with higher values before the extinction event, and lower values after the event (Fig. 6). The overall trend shows a shortening of on average 3-5 μm , which is substantially larger than the variability within one specimen. The trend is also gradual, in contrast to the facies changes, which are abrupt, and the shorter processes are thus not directly linked with stratification. Instead, the shortening of the processes could be interpreted as a lowering in salinity during the extinction event. Within the 2m interval including the extinction interval (-1 – +1m) there is also a small, offset in body size between samples from bioturbated and laminated rocks, however, this difference is not consistent when considering the full record. The body size of some dinocysts has been found to vary with temperature and salinity (e.g. Ellegaard et al., 2002; Mertens et al., 2012), however, the relation has not been well studied. Possibly low oxygen or salinity conditions or increased nutrient availability influenced acritarch body size in this interval. Runoff, lower salinity, and salinity stratification together can explain the observed changes in palynofacies and acritarch records. In addition, transport of acritarchs with shorter processes from near shore environment into deeper marine environment could also result in on average shorter processes. However, this would result in a bimodal distribution of process length within one interval (near shore specimens with shorter processes, and deep-water specimens with longer processes). Instead process length, although variable within each interval, changes gradually (see also Fig. S1). The changed environmental conditions continued through the aftermath of the biotic crisis, as shown by persistently low process lengths to the end of the study interval (Fig. 6). Meanwhile, the ongoing marine transgression likely resulted in the shoreward migration of oxygen deficient waters which explain the development of permanently anoxic conditions higher up in the Wordie Creek Formation (over 0.6-0.7 m from the Fm boundary) (Mettam et al., 2017).

The development of widespread anoxia in the late Permian is usually explained by an expansion of anoxic deep waters onto the shelf (e.g. Grasby and Beauchamp, 2009). However, increased runoff and the development of estuarine circulation provide an alternative explanation for the development of anoxia in some shallow marine environments. Furthermore, low salinity is known to negatively impact biomass and size of modern marine invertebrates (e.g. Westerborg et al., 2002), and, along with higher temperatures and hypoxia, might also be a contributing factor in the size reduction of marine organisms recorded in the aftermath of the late Permian extinction event, such as observed for the bivalve *Claraia* the Permian-Triassic section of East-Greenland (Twitchett, 2007). Low salinity conditions have previously been invoked to explain the dominance of the brachiopod lingulid in post-extinction ecosystems (Zonneveld et al., 2007), because they are able to tolerate a wide range of salinities as well as hypoxia (e.g. Hammen and Lum, 1977). Lingulid fossils are found in many Permian-Triassic (shallow) marine sections (e.g. Peng et al., 2007) and the lowering of salinities in shallow marine settings and spreading anoxia provided ecological space for the lingulids (Peng et al., 2007; Rodland and Bottjer, 2001). It has been suggested that rising sea water temperatures in the Tethys, resulted in strengthened monsoonal activity (e.g. Winguth and Winguth, 2012) and enhanced precipitation and runoff in the areas surrounding the Tethys (e.g. Parrish et al., 1982). Whether this would have had an effect on the study site is questionable, because of its distance to the Tethys and relatively sheltered, inland position. Possibly river systems existed which brought freshwater to the Greenland-Norway basin from the South. It is also possible that rainfall increased locally. Mettam et al., (2017) speculated that changes in circulation patterns may have resulted

in onshore winds bringing moist air to the study site. In addition vegetation destruction and soil erosion may also have contributed to enhanced runoff.

5.3 Sea water temperature

Besides salinity, increasing water temperatures can also affect process length in dinocysts (e.g. Mertens et al., 2009, 2012) but this relationship is not always evident (e.g. Ellegaard et al., 2002). Sea water temperature reconstructions for the late Permian and Early Triassic exist mainly from carbonate rich sections originating in the Tethys Ocean (e.g. Joachimski et al., 2012; Schobben et al., 2014; Sun et al., 2012). These reconstructions indicate increasing temperatures during the extinction event, and maximum temperatures are reached in the Early Triassic (e.g. Joachimski et al., 2012; Kearsley et al., 2009; Schobben et al., 2014; Sun et al., 2012). Since no water temperature reconstructions exist for the Greenland-Norway basin, at this time, it is not possible to exclude the effects of rising water temperatures on the acritarch morphology. Increasing water temperatures might be partly responsible for decreasing process length in acritarchs, however, a rising sea-level in combination with rising temperatures are not able to explain the changes in the acritarch assemblages, which indicate a shift from more open marine to near-shore conditions. Increased runoff cannot only explain the reconstructed changes in palynofacies and acritarch records, but in addition, a reduction in salinity also has significant implications for palaeotemperature reconstructions calculated from the oxygen isotopes of carbonates. Most Permian-Triassic temperature records are from the Tethys or surrounding areas, where monsoon activity has been proposed to increase (Winguth and Winguth, 2012) and thus salinity is expected to change as well. Permian-Triassic oxygen isotope data for palaeotemperature estimates have been derived from brachiopod shells (Kearsley et al., 2009) or conodont apatite (Joachimski et al., 2012; Schobben et al., 2014), with all studies concluding that temperature rose through the extinction event and that Early Triassic seas were 'lethally hot' (Sun et al., 2012). Oxygen isotope values partially reflect seawater salinity, although this is generally ignored in palaeotemperature studies, because there is currently no independent proxy of salinity change, and so it is assumed that salinity remained constant. If salinity was reduced in shelf seas due to hydrological changes (e.g. enhanced precipitation and run-off), as it appears for East Greenland at least, then all of these studies may have significantly over-estimated Early Triassic temperatures. The actual temperature rise associated with the extinction event would have been lower and below 'lethal' levels, which is more consistent with fossil evidence that the oceans were not completely devoid of life.

6. Conclusions

The highest resolution palynological sampling yet attempted for the Fiskegrav location of central Jameson Land has shown significant, millennial-scale changes in marine and terrestrial environments. The biotic crisis, defined by a peak in the spore/pollen ratio, which indicates widespread disruption and collapse of the terrestrial flora, postdates the onset of the carbon-isotope excursion. The spore/pollen peak spans 0.8 m of section, which, on current age estimates, gives an estimation of 1600 to 8000 years for the ecosystem collapse. This is much shorter than previous estimations. The onset of the biotic crisis does not appear to coincide with any obvious

changes in lithology or sedimentary facies, and deposition of the shallow marine shelf sediments appears to have taken place under oxygenated waters. During the latter stages of the biotic crisis, laminated beds begin to appear, indicating periodic anoxic deposition. These laminated rocks contain palynological evidence for a more near-shore setting, which contradicts the widely accepted evidence that globally sea-level was rising during the extinction event. A preferred alternative explanation, consistent with palynological assemblages, is that enhanced runoff, water column stratification and enhanced primary productivity led to the development of anoxic bottom waters. Enhanced runoff would lead to elevated freshwater flux into shallow shelf seas, which would have led to the development of a freshwater wedge, stratification and a reduction in salinity. Acritarch process length is considered here to be a proxy for seawater salinity, and supports these inferred changes. Increased runoff did not immediately lead to anoxia, possibly because precipitation gradually increased during the extinction event until the freshwater flow was large enough to cause water column stratification. Increasing sea water temperatures may have also affected acritarch morphology, and partially be responsible for the reduced process length. However, rising temperatures alone cannot explain the reconstructed changes in the palynofacies and acritarch records. In fact, sea water temperature reconstructions may overestimate the rise in water temperatures during the extinction event, since possible changes in salinity are not included in the calculations.

7. Data availability. The data reported in this paper is available in tables in the supplementary files.

Author contributions. WMK designed the study. RJT provided material. EEvS analysed the samples for palynofacies and palynomorph content and performed measurements on acritarchs. EEvS wrote the paper with input from WMK and RJT.

Competing interests. The authors declare that they have no conflict of interest.

Acknowledgements

This work was funded by the Norwegian Research Council, project 234005, The Permian/Triassic evolution of the Timan-Pechora and Barents Sea Basins. We thank B.L. Berg and M.S. Naoroz for technical support. Samples were collected by RJT, who thanks G. Cuny and the Danish National Research Foundation for logistic and financial support.

References

Algeo, T. J. and Twitchett, R. J.: Anomalous Early Triassic sediment fluxes due to elevated weathering rates and their biological consequences, *Geology*, 38(11), 1023–1026, doi:10.1130/G31203.1, 2010.

412 Algeo, T. J., Heckel, P. H., Maynard, J. B., Blakey, R. and Rowe, H.: Modern and ancient epeiric seas and the
 413 super-estuarine circulation model of marine anoxia, *Dynamics of Epeiric seas: sedimentological, paleontological*
 414 *and geochemical perspectives*. Geological Association Canada Special Publication, 7–38, 2008.

415 Balme, B. E.: Palynology of Permian-Triassic boundary beds at Kap Stosch, East Greenland, *Nyt nordisk forlag*,
 416 200(6), 1979.

417 Benton, M. J. and Twitchett, R. J.: How to kill (almost) all life: the end-Permian extinction event, *Trends in*
 418 *Ecology & Evolution*, 18(7), 358–365, doi:10.1016/S0169-5347(03)00093-4, 2003.

419 Bond, D. P. G. and Wignall, P. B.: Pyrite framboid study of marine Permian–Triassic boundary sections: A
 420 complex anoxic event and its relationship to contemporaneous mass extinction, *GSA Bulletin*, 122(7–8), 1265–
 421 1279, doi:10.1130/B30042.1, 2010.

422 Bouimetarhan, I., Marret, F., Dupont, L. and Zonneveld, K.: Dinoflagellate cyst distribution in marine surface
 423 sediments off West Africa (17–6°N) in relation to sea-surface conditions, freshwater input and seasonal coastal
 424 upwelling, *Mar. Micropaleontol.*, 71(3–4), 113–130, doi:10.1016/j.marmicro.2009.02.001, 2009.

425 Burgess, S. D. and Bowring, S. A.: High-precision geochronology confirms voluminous magmatism before,
 426 during, and after Earth’s most severe extinction, *Science Advances*, 1(7), e1500470,
 427 doi:10.1126/sciadv.1500470, 2015.

428 Burgess, S. D., Muirhead, J. D. and Bowring, S. A.: Initial pulse of Siberian Traps sills as the trigger of the end-
 429 Permian mass extinction, *Nat. Commun.*, 8(1), 164, doi:10.1038/s41467-017-00083-9, 2017.

430 Clapham, M. E. and Payne, J. L.: Acidification, anoxia, and extinction: A multiple logistic regression analysis of
 431 extinction selectivity during the Middle and Late Permian, *Geology*, 39(11), 1059–1062, doi:10.1130/G32230.1,
 432 2011.

433 Colbath, G. K. and Grenfell, H. R.: Review of biological affinities of Paleozoic acid-resistant, organic-walled
 434 eukaryotic algal microfossils (including “acritarchs”), *Rev. Palaeobot. Palyno.*, 86(3–4), 287–314,
 435 doi:10.1016/0034-6667(94)00148-D, 1995.

436 Cui, Y. and Kump, L. R.: Global warming and the end-Permian extinction event: Proxy and modeling
 437 perspectives, *Earth-Science Reviews*, 149, 5–22, doi:10.1016/j.earscirev.2014.04.007, 2015.

438 Devillers, R. and de Vernal, A.: Distribution of dinoflagellate cysts in surface sediments of the northern North
 439 Atlantic in relation to nutrient content and productivity in surface waters, *Mar. Geol.*, 166(1), 103–124,
 440 doi:10.1016/S0025-3227(00)00007-4, 2000.

441 Ellegaard, M.: Variations in dinoflagellate cyst morphology under conditions of changing salinity during the last
 442 2000 years in the Limfjord, Denmark, *Rev. Palaeobot. Palyno.*, 109(1), 65–81, doi:10.1016/S0034-
 443 6667(99)00045-7, 2000.

444 Ellegaard, M., Lewis, J. and Harding, I.: Cyst–theca relationship, life cycle, and effects of temperature and
 445 salinity on the cyst morphology of *Gonyaulax Baltica* Sp. Nov. (dinophyceae) from the Baltic Sea Area, *J.*
 446 *Phycol.*, 38(4), 775–789, doi:10.1046/j.1529-8817.2002.01062.x, 2002.

447 Evitt, W. R.: A discussion and proposals concerning fossil dinoflagellates, hystrichospheres, and acritarchs, *I*,
 448 *PNAS*, 49(2), 158–164, 1963.

449 Fischer, A. G.: Brackish oceans as the cause of the Permo-Triassic marine faunal crisis, in *Problems in*
 450 *Palaeoclimatology*, edited by A. E. M. Nairn, pp. 566–574, Interscience, London., 1964.

451 Grard, A., François, L. M., Dessert, C., Dupré, B. and Goddérès, Y.: Basaltic volcanism and mass extinction at
 452 the Permo-Triassic boundary: Environmental impact and modeling of the global carbon cycle, *Earth and*
 453 *Planetary Science Letters*, 234(1), 207–221, doi:10.1016/j.epsl.2005.02.027, 2005.

454 Grasby, S. E. and Beauchamp, B.: Latest Permian to Early Triassic basin-to-shelf anoxia in the Sverdrup Basin,
 455 Arctic Canada, *Chem. Geol.*, 264(1–4), 232–246, doi:10.1016/j.chemgeo.2009.03.009, 2009.

456 Grasby, S. E., Beauchamp, B., Bond, D. P. G., Wignall, P., Talavera, C., Galloway, J. M., Piepjohn, K.,
 457 Reinhardt, L. and Blomeier, D.: Progressive environmental deterioration in northwestern Pangea leading to the
 458 latest Permian extinction, *Geol. Soc. Am. Bull.*, B31197.1, doi:10.1130/B31197.1, 2015.

459 Hallam, A. and Cohen, J. M.: The Case for Sea-Level Change as a Dominant Causal Factor in Mass Extinction
 460 of Marine Invertebrates [and Discussion], *Philos. T. Roy. Soc. B*, 325(1228), 437–455, doi:10.2307/2396934,
 461 1989.

462 Hammen, C. S. and Lum, S. C.: Salinity tolerance and pedicle regeneration of *Lingula*, *J. Paleontol.*, 51(3), 548–
 463 551, 1977.

464 Hotinski, R. M., Bice, K. L., Kump, L. R., Najjar, R. G. and Arthur, M. A.: Ocean stagnation and end-Permian
 465 anoxia, *Geology*, 29(1), 7–10, doi:10.1130/0091-7613(2001)029<0007:OSAEPA>2.0.CO;2, 2001.

466 Isozaki, Y.: Permo-Triassic Boundary Superanoxia and Stratified Superocean: Records from Lost Deep Sea,
 467 *Science*, 276(5310), 235–238, doi:10.1126/science.276.5310.235, 1997.

468 Jansonius, J.: Palynology of permian and triassic sediments, Peace River area, Western Canada, *Palaeontogr.*
 469 *Abt. B*, 35–98, 1962.

470 Joachimski, M. M., Lai, X., Shen, S., Jiang, H., Luo, G., Chen, B., Chen, J. and Sun, Y.: Climate warming in the
 471 latest Permian and the Permian–Triassic mass extinction, *Geology*, 40(3), 195–198, doi:10.1130/G32707.1,
 472 2012.

473 Kearsy, T., Twitchett, R. J., Price, G. D. and Grimes, S. T.: Isotope excursions and palaeotemperature estimates
 474 from the Permian/Triassic boundary in the Southern Alps (Italy), *Palaeogeogr. Palaeocl.*, 279(1–2), 29–40,
 475 doi:10.1016/j.palaeo.2009.04.015, 2009.

476 Korte, C. and Kozur, H. W.: Carbon-isotope stratigraphy across the Permian–Triassic boundary: A review, J.
 477 Asian Earth Sci., 39(4), 215–235, doi:10.1016/j.jseaes.2010.01.005, 2010.

478 Lei, Y., Servais, T., Feng, Q. and He, W.: The spatial (nearshore–offshore) distribution of latest Permian
 479 phytoplankton from the Yangtze Block, South China, Palaeogeogr. Palaeoclimatol., 363–364, 151–162,
 480 doi:10.1016/j.palaeo.2012.09.010, 2012.

481 Lei, Y., Servais, T., Feng, Q. and He, W.: Latest Permian acritarchs from South China and the
 482 Micrhystridium/Veryhachium complex revisited, Palynology, 37(2), 325–344,
 483 doi:10.1080/01916122.2013.793625, 2013a.

484 Lei, Y., Servais, T. and Feng, Q.: The diversity of the Permian phytoplankton, Rev. Palaeobot. Palynol., 198,
 485 145–161, doi:10.1016/j.revpalbo.2013.03.004, 2013b.

486 Li, J., Servais, T., Yan, K. and Zhu, H.: A nearshore–offshore trend in acritarch distribution from the Early–
 487 Middle Ordovician of the Yangtze Platform, South China, Rev. Palaeobot. Palynol., 130(1–4), 141–161,
 488 doi:10.1016/j.revpalbo.2003.12.005, 2004.

489 Looy, C. V., Twitchett, R. J., Dilcher, D. L., Van Konijnenburg-Van Cittert, J. H. and Visscher, H.: Life in the
 490 end-Permian dead zone, PNAS, 98(14), 7879–7883, 2001.

491 McGhee, G. R., Sheehan, P. M., Bottjer, D. J. and Droser, M. L.: Ecological ranking of Phanerozoic
 492 biodiversity crises: The Serpukhovian (early Carboniferous) crisis had a greater ecological impact than the end-
 493 Ordovician, Geology, 40(2), 147–150, doi:10.1130/G32679.1, 2012.

494 Mertens, K. N., Ribeiro, S., Bouimetarhan, I., Caner, H., Combourieu Nebout, N., Dale, B., De Vernal, A.,
 495 Ellegaard, M., Filipova, M., Godhe, A., Goubert, E., Grøsfjeld, K., Holzwarth, U., Kotthoff, U., Leroy, S. A. G.,
 496 Londeix, L., Marret, F., Matsuoka, K., Mudie, P. J., Naudts, L., Peña-Manjarrez, J. L., Persson, A., Popescu, S.-
 497 M., Pospelova, V., Sangiorgi, F., van der Meer, M. T. J., Vink, A., Zonneveld, K. A. F., Vercauteren, D.,
 498 Vlassenbroeck, J. and Louwye, S.: Process length variation in cysts of a dinoflagellate, Lingulodinium
 499 machaerophorum, in surface sediments: Investigating its potential as salinity proxy, Mar. Micropaleontol., 70(1–
 500 2), 54–69, doi:10.1016/j.marmicro.2008.10.004, 2009.

501 Mertens, K. N., Dale, B., Ellegaard, M., Jansson, I.-M., Godhe, A., Kremp, A. and Louwye, S.: Process length
 502 variation in cysts of the dinoflagellate Protoceratium reticulatum, from surface sediments of the Baltic–
 503 Kattegat–Skagerrak estuarine system: a regional salinity proxy, Boreas, 40(2), 242–255, doi:10.1111/j.1502-
 504 3885.2010.00193.x, 2011.

505 Mertens, K. N., Bringué, M., Van Nieuwenhove, N., Takano, Y., Pospelova, V., Rochon, A., De Vernal, A.,
 506 Radi, T., Dale, B., Patterson, R. T., Weckström, K., Andrén, E., Louwye, S. and Matsuoka, K.: Process length
 507 variation of the cyst of the dinoflagellate Protoceratium reticulatum in the North Pacific and Baltic-Skagerrak
 508 region: calibration as an annual density proxy and first evidence of pseudo-cryptic speciation, J. Quaternary Sci.,
 509 27(7), 734–744, doi:10.1002/jqs.2564, 2012.

510 Mettam, C., Zerkle, A. L., Claire, M. W., Izon, G., Junium, C. J. and Twitchett, R. J.: High-frequency
511 fluctuations in redox conditions during the latest Permian mass extinction, *Palaeogeogr. Palaeoclimatol.*,
512 doi:10.1016/j.palaeo.2017.06.014, 2017.

513 Mudie, P. J., Aksu, A. E. and Yasar, D.: Late Quaternary dinoflagellate cysts from the Black, Marmara and
514 Aegean seas: variations in assemblages, morphology and paleosalinity, *Mar. Micropaleontol.*, 43(1–2), 155–178,
515 doi:10.1016/S0377-8398(01)00006-8, 2001.

516 Mudie, P. J., Rochon, A., Aksu, A. E. and Gillespie, H.: Dinoflagellate cysts, freshwater algae and fungal spores
517 as salinity indicators in Late Quaternary cores from Marmara and Black seas, *Mar. Geol.*, 190(1), 203–231,
518 doi:10.1016/S0025-3227(02)00348-1, 2002.

519 Pacton, M., Gorin, G. E. and Vasconcelos, C.: Amorphous organic matter — Experimental data on formation
520 and the role of microbes, *Rev. Palaeobot. Palynol.*, 166(3–4), 253–267, doi:10.1016/j.revpalbo.2011.05.011,
521 2011.

522 Parrish, J. T., Ziegler, A. M. and Scotese, C. R.: Rainfall patterns and the distribution of coals and evaporites in
523 the Mesozoic and Cenozoic, *Palaeogeogr. Palaeoclimatol.*, 40(1), 67–101, doi:10.1016/0031-0182(82)90085-2, 1982.

524 Peng, Y., Shi, G. R., Gao, Y., He, W. and Shen, S.: How and why did the Lingulidae (Brachiopoda) not only
525 survive the end-Permian mass extinction but also thrive in its aftermath?, *Palaeogeogr. Palaeoclimatol.*, 252(1–2),
526 118–131, doi:10.1016/j.palaeo.2006.11.039, 2007.

527 Piasecki, S.: Preliminary palynostratigraphy of the Permian-Lower Triassic sediments in Jameson Land and
528 Scoresby Land, East Greenland, *B. Geol. Soc. Denmark*, 32, 139–144, 1984.

529 Pospelova, V., Chmura, G. L. and Walker, H. A.: Environmental factors influencing the spatial distribution of
530 dinoflagellate cyst assemblages in shallow lagoons of southern New England (USA), *Rev. Palaeobot. Palynol.*,
531 128(1–2), 7–34, doi:10.1016/S0034-6667(03)00110-6, 2004.

532 Rodland, D. L. and Bottjer, D. J.: Biotic Recovery from the End-Permian Mass Extinction: Behavior of the
533 Inarticulate Brachiopod *Lingula* as a Disaster Taxon, *PALAIOS*, 16(1), 95–101, doi:10.1669/0883-
534 1351(2001)016<0095:BRFTEP>2.0.CO;2, 2001.

535 Sarjeant, W. A. S.: Acritarchs and tasmanitids from the Chhidru Formation, uppermost Permian of West
536 Pakistan, *Stratigraphic Boundary Problems: Permian and Triassic of West Pakistan*, *Spec. Publ.* 4, 277–304,
537 1970.

538 Sarjeant, W. A. S. and Stancliffe, R. P. W.: The *Micrhystridium* and *Veryhachium* Complexes (Acritarcha:
539 *Acanthomorpha* and *Polygonomorpha*): A Taxonomic Reconsideration, *Micropaleontology*, 40(1), 1–77,
540 doi:10.2307/1485800, 1994.

541 Schobben, M., Joachimski, M. M., Korn, D., Leda, L. and Korte, C.: Palaeotethys seawater temperature rise and
542 an intensified hydrological cycle following the end-Permian mass extinction, *Gondwana Res.*, 26(2), 675–683,
543 doi:10.1016/j.gr.2013.07.019, 2014.

544 Sephton, M. A., Looy, C. V., Brinkhuis, H., Wignall, P. B., De Leeuw, J. W. and Visscher, H.: Catastrophic soil
545 erosion during the end-Permian biotic crisis, *Geology*, 33(12), 941–944, 2005.

546 Servais, T., Stricanne, L., Montenari, M. and Pross, J.: Population dynamics of galeate acritarchs at the
547 Cambrian–Ordovician transition in the Algerian Sahara, *Palaeontology*, 47(2), 395–414, doi:10.1111/j.0031-
548 0239.2004.00367.x, 2004.

549 Shen, J., Lei, Y., Algeo, T. J., Feng, Q., Servais, T., Yu, J. and Zhou, L.: Volcanic effects on microplankton
550 during the Permian-Triassic transition (Shangsi and Xinmin, South China), *PALAIOS*, 28(8), 552–567,
551 doi:10.2110/palo.2013.p13-014r, 2013.

552 Sluijs, A. and Brinkhuis, H.: A dynamic climate and ecosystem state during the Paleocene-Eocene Thermal
553 Maximum: inferences from dinoflagellate cyst assemblages on the New Jersey Shelf, *Biogeosciences*, 6(8),
554 1755–1781, doi:10.5194/bg-6-1755-2009, 2009.

555 Stemmerik, L. A. R. S., Bendix-Almgreen, S. E. and Piasecki, S.: The Permian–Triassic boundary in central
556 East Greenland: past and present views." *Bulletin of the Geological Society of Denmark*, B. Geol. Soc.
557 Denmark, 48(2), 159–167, 2001.

558 Stevens, C. H.: Was development of brackish oceans a factor in Permian extinctions?, *Geol. Soc. Am. Bull.*,
559 88(1), 133–138, doi:10.1130/0016-7606(1977)88<133:WDOBOA>2.0.CO;2, 1977.

560 Stricanne, L., Munnecke, A., Pross, J. and Servais, T.: Acritarch distribution along an inshore–offshore transect
561 in the Gorstian (lower Ludlow) of Gotland, Sweden, *Rev. Palaeobot. Palyno.*, 130(1–4), 195–216,
562 doi:10.1016/j.revpalbo.2003.12.007, 2004.

563 Sun, Y., Joachimski, M. M., Wignall, P. B., Yan, C., Chen, Y., Jiang, H., Wang, L. and Lai, X.: Lethally hot
564 temperatures during the Early Triassic greenhouse, *Science*, 338(6105), 366–370, doi:10.1126/science.1224126,
565 2012.

566 Surlyk, F., Piasecki, S., Rolle, F., Stemmerik, L., Thomsen, E. and Wrang, P.: The Permian base of East
567 Greenland, in *Petroleum Geology of the North European Margin*, edited by A. M. Spencer, pp. 303–315,
568 Springer Netherlands., 1984.

569 Svensen, H., Planke, S., Polozov, A. G., Schmidbauer, N., Corfu, F., Podladchikov, Y. Y. and Jamtveit, B.:
570 Siberian gas venting and the end-Permian environmental crisis, *Earth Planet. Sc. Lett.*, 277(3–4), 490–500,
571 doi:10.1016/j.epsl.2008.11.015, 2009.

572 Tappan, H. and Loeblich, A. R.: Evolution of the oceanic plankton, *Earth-Sci. Rev.*, 9(3), 207–240,
573 doi:10.1016/0012-8252(73)90092-5, 1973.

574 Twitchett, R. J.: The Lilliput effect in the aftermath of the end-Permian extinction event, *Palaeogeogr. Palaeocl.*,
575 252(1–2), 132–144, doi:10.1016/j.palaeo.2006.11.038, 2007.

576 Twitchett, R. J., Looy, C. V., Morante, R., Visscher, H. and Wignall, P. B.: Rapid and synchronous collapse of
577 marine and terrestrial ecosystems during the end-Permian biotic crisis, *Geology*, 29(4), 351–354,
578 doi:10.1130/0091-7613(2001)029<0351:RASCOM>2.0.CO;2, 2001.

579 Tyson, R.: *Sedimentary Organic Matter: Organic facies and palynofacies*, 1995 edition., Springer., 1995.

580 Vernal, A. de, Hillaire-Marcel, C., Turon, J.-L. and Matthiessen, J.: Reconstruction of sea-surface temperature,
581 salinity, and sea-ice cover in the northern North Atlantic during the last glacial maximum based on dinocyst
582 assemblages, *Can. J. Earth Sci.*, 37(5), 725–750, doi:10.1139/e99-091, 2000.

583 Westerbom, M., Kilpi, M. and Mustonen, O.: Blue mussels, *Mytilus edulis*, at the edge of the range: population
584 structure, growth and biomass along a salinity gradient in the north-eastern Baltic Sea, *Mar. Biol.*, 140(5), 991–
585 999, doi:10.1007/s00227-001-0765-6, 2002.

586 Wignall, P. B. and Hallam, A.: Anoxia as a cause of the Permian/Triassic mass extinction: facies evidence from
587 northern Italy and the western United States, *Palaeogeogr. Palaeocl.*, 93(1), 21–46, doi:10.1016/0031-
588 0182(92)90182-5, 1992.

589 Wignall, P. B. and Twitchett, R. J.: Oceanic anoxia and the end Permian mass extinction, *Science*, 272(5265),
590 1155, 1996.

591 Wignall, P. B. and Twitchett, R. J.: Permian–Triassic sedimentology of Jameson Land, East Greenland: incised
592 submarine channels in an anoxic basin, *J. Geol. Soc.*, 159(6), 691–703, doi:10.1144/0016-764900-120, 2002.

593 Winguth, A. and Winguth, C.: Precession-driven monsoon variability at the Permian–Triassic boundary —
594 Implications for anoxia and the mass extinction, *Global. Planet. Change*, 105, 160–170,
595 doi:10.1016/j.gloplacha.2012.06.006, 2012.

596 Yin, H., Ed.: *The Palaeozoic-Mesozoic boundary, candidates of Global Stratotype Section and Point of the*
597 *Permian-Triassic boundary*, China University of Geosciences Press, Wuhan., 1996.

598 Zonneveld, J.-P., Beatty, T. W. and Pemberton, S. G.: Lingulide Brachiopods and the Trace Fossil *Lingulichnus*
599 *from the Triassic of Western Canada: Implications for Faunal Recovery After the End-Permian Mass Extinction*,
600 *PALAIOS*, 22(1), 74–97, doi:10.2110/palo.2005.p05-103r, 2007.

601 Zonneveld, K. A. F., Marret, F., Versteegh, G. J. M., Bogus, K., Bonnet, S., Bouimetarhan, I., Crouch, E., de
602 Vernal, A., Elshanawany, R., Edwards, L., Esper, O., Forke, S., Grøsfjeld, K., Henry, M., Holzwarth, U., Kielt,
603 J.-F., Kim, S.-Y., Ladouceur, S., Ledu, D., Chen, L., Limoges, A., Londeix, L., Lu, S.-H., Mahmoud, M. S.,
604 Marino, G., Matsouka, K., Matthiessen, J., Mildenhall, D. C., Mudie, P., Neil, H. L., Pospelova, V., Qi, Y., Radi,
605 T., Richerol, T., Rochon, A., Sangiorgi, F., Solignac, S., Turon, J.-L., Verleye, T., Wang, Y., Wang, Z. and
606 Young, M.: Atlas of modern dinoflagellate cyst distribution based on 2405 data points, *Rev. Palaeobot. Palyno.*,
607 191, 1–197, doi:10.1016/j.revpalbo.2012.08.003, 2013.

608

609

610

Figure 1. Modern map of Jameson Land, East Greenland (adapted from Piasecki, 1984). The location of the studied section is indicated with a red circle. The right panel show the lithology of the Jameson Land section and sample depths. (* spore-peak after Looy et al., 2001, marine collapse after Twitchett et al., 2001).

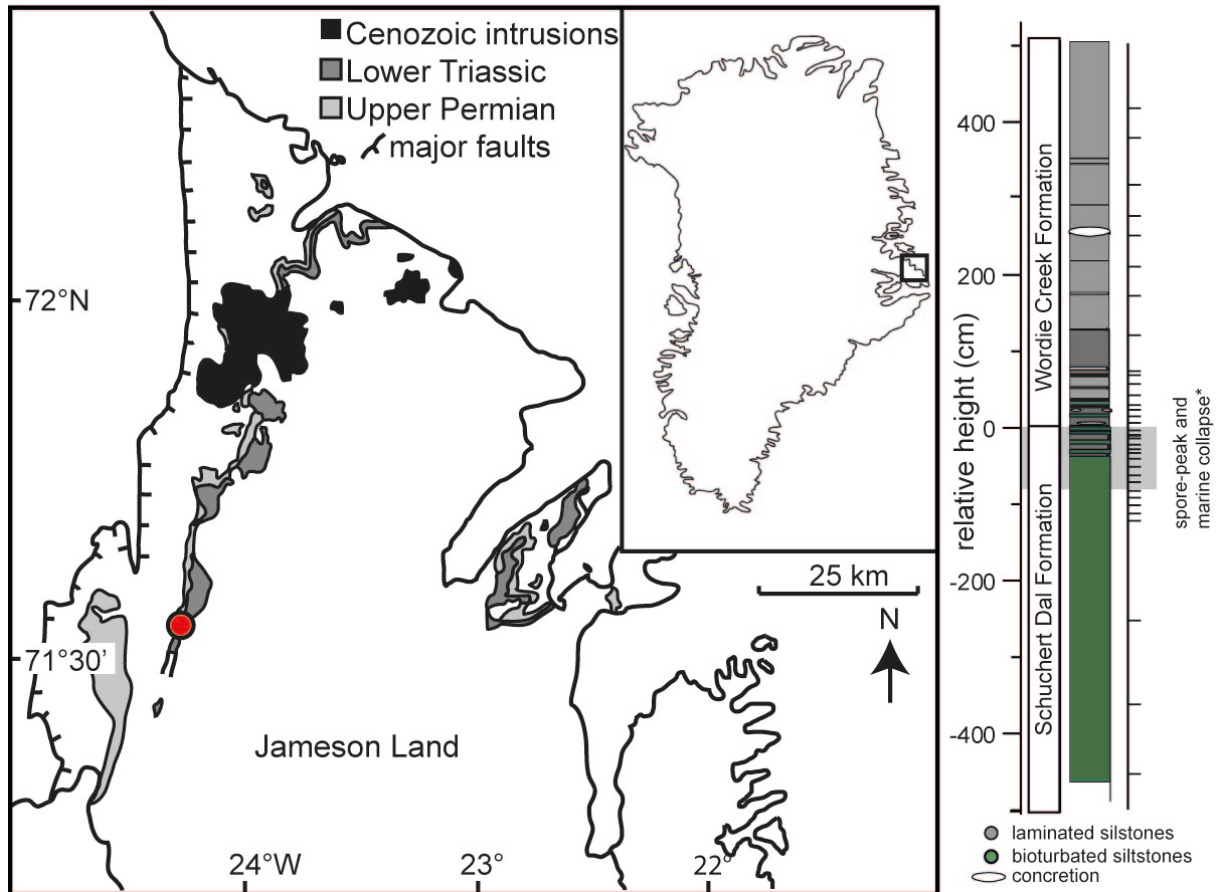


Figure. 2. Change in major groups of palynofacies. AOM= amorphous organic matter. The grey shaded box highlights the biotic crisis as defined by the high spore/pollen ratios, which are indicative for the disappearance of forest communities. Green shading indicates data from bioturbated rocks; grey shading indicates data from laminated rocks. Grey horizontal bar indicates the extinction interval, based on high spore: pollen ratios.

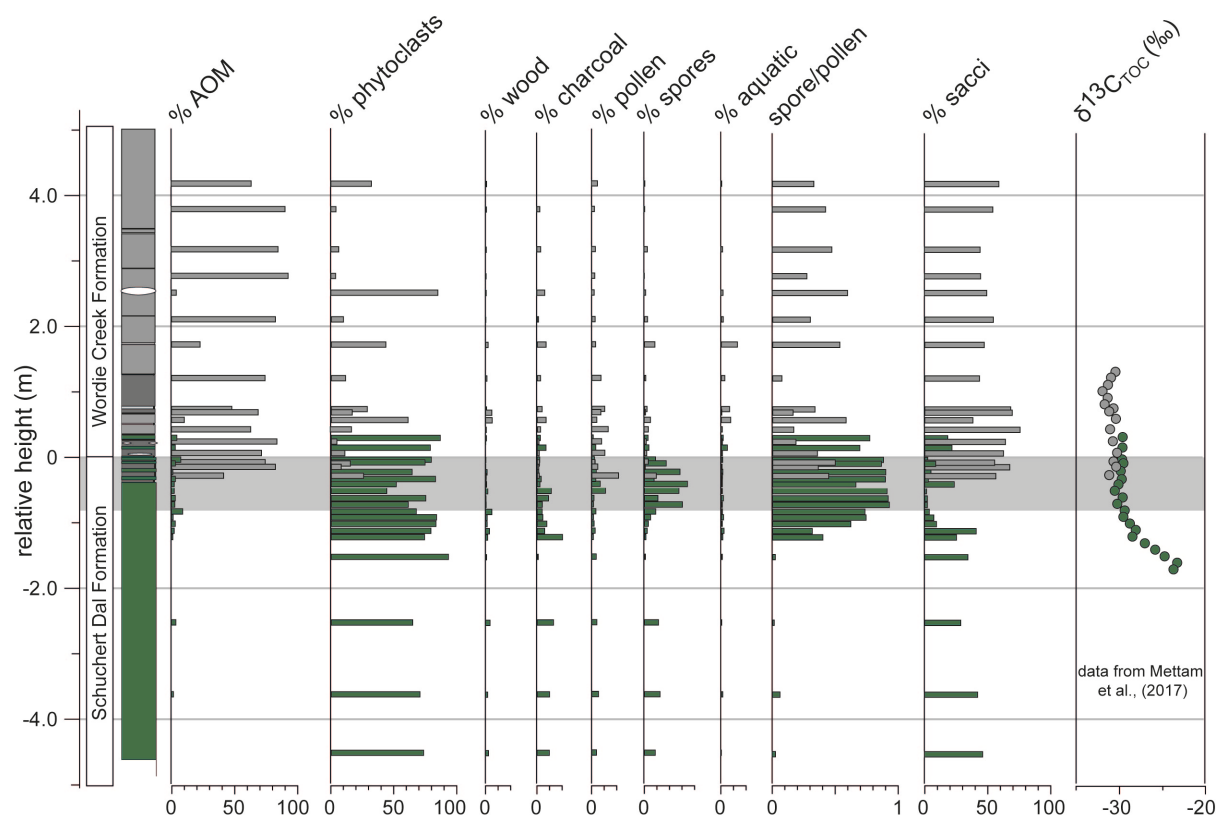


Figure 3. Aquatic palynomorphs plate. A) *M. pentagonale* – group, B) *V. laidii* - group C) *Cymatiosphaera* sp. D) and E) leiospheres F)-I) *M. breve* -group J) *M. pentagonale* - group K)-M) *M. breve* - group N) *Cymatiosphaera* sp. O) and P) *M. breve* -group

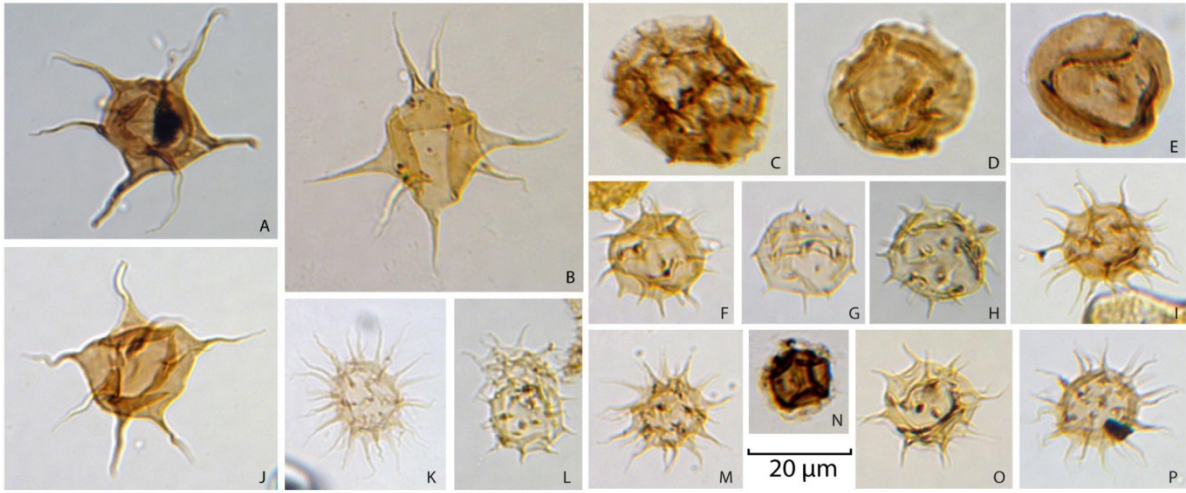
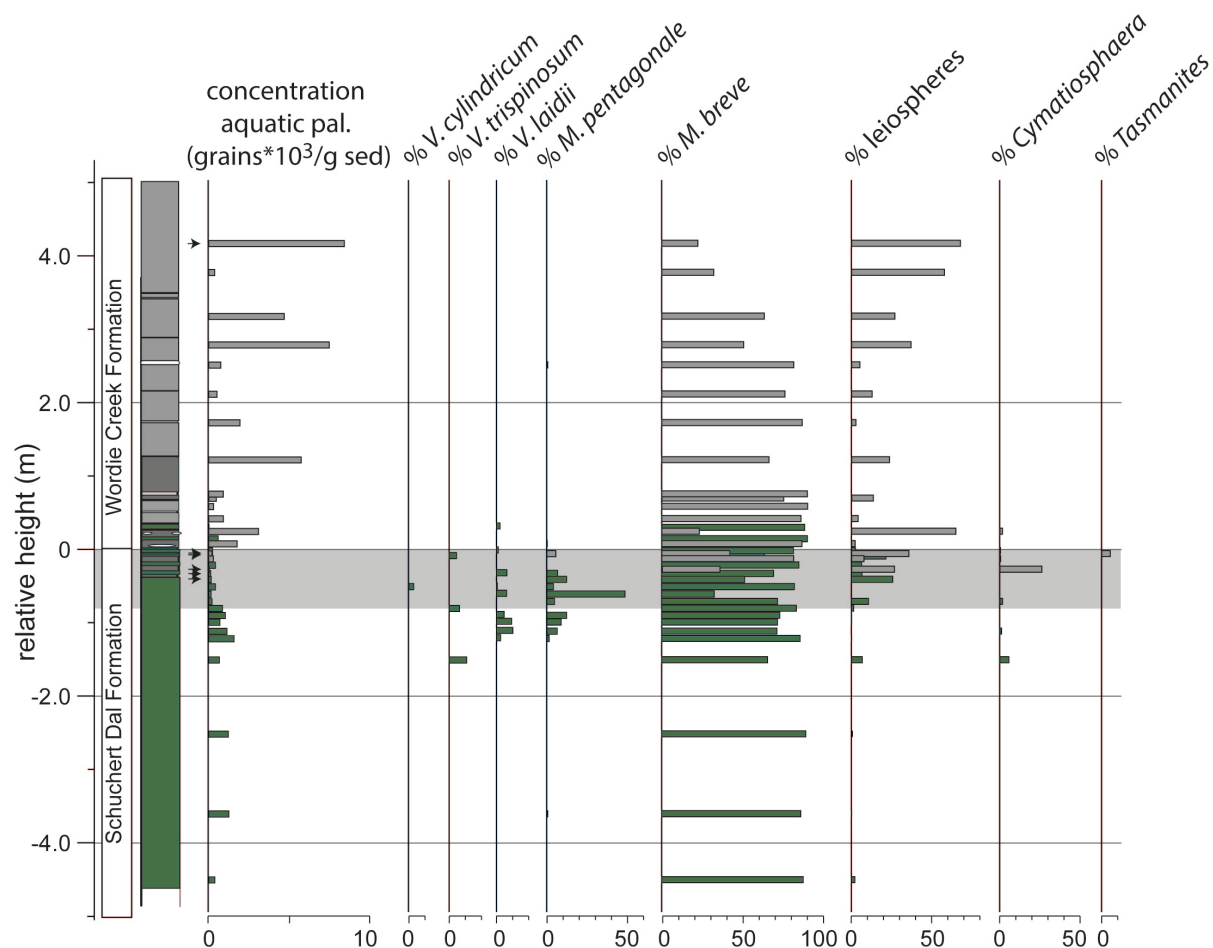
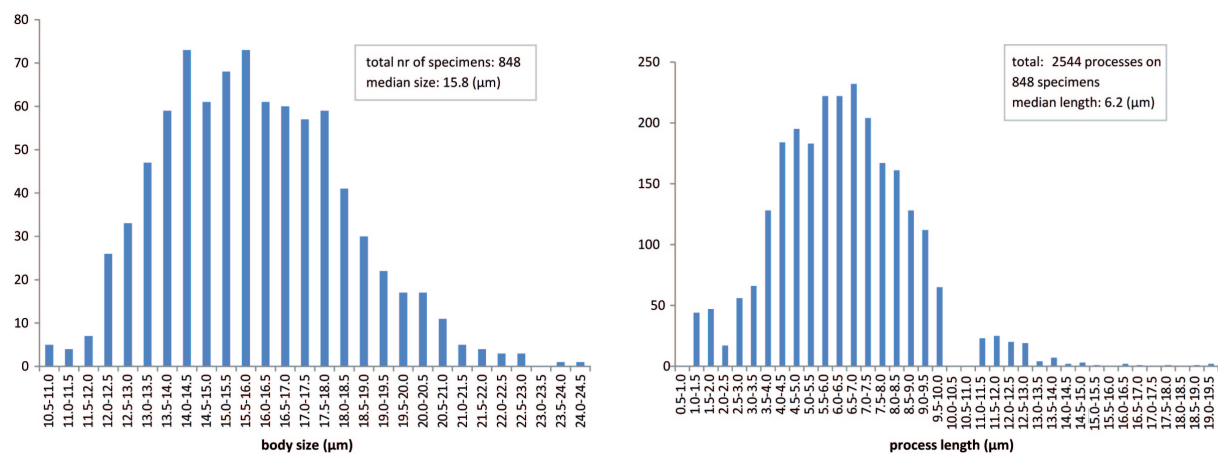


Figure 4. Aquatic palynomorphs. The figure shows concentration of all aquatic palynomorphs and relative abundance specific acritarch and prasinophyte groups. Arrow indicate intervals with low counts (<20). Green shading indicates data from bioturbated rocks; grey shading indicates data from laminated rocks. Grey horizontal bar indicates the extinction interval, based on high spore: pollen ratios.



646 **Figure 5.** Size-frequency of body diamter (left) and proces length (right).



647

648

649

Figure 6. Changes in acritarch abundance and morphology. In the panel on the left are the main groups of aquatic palynomorphs summarized. On the right: body size, process length, and process length relative to body size. Where are low counts? Green shading indicates data from bioturbated rocks; grey shading indicates data from laminated rocks. The grey bar indicates the extinction interval, based on high spore:pollen ratios. The five small black arrows indicate in which samples the number of specimens used for measurements was low (4-16 specimens). Grey horizontal bar indicates the extinction interval, based on high spore: pollen ratios.

